IEEE Access
Multidisciplinary | Rapid Review | Open Access Journal

Received June 27, 2019, accepted July 19, 2019, date of publication July 29, 2019, date of current version August 23, 2019.

Digital Object Identifier 10.1109/ACCESS.2019.2931729

The Explicit Tuning Investigation and Validation of a Full Kalman Filter-Based Tracking Loop in GNSS Receivers

XINHUA TANG[1], XIN CHEN[2], ZHONGHAI PEI[3], AND PENG WANG[3]

[1]Key Laboratory of Micro-Inertial Instrument and Advanced Navigation Technology, Ministry of Education, School of Instrument Science and Engineering, Southeast University, Nanjing 210096, China
[2]School of Electronic Information and Electrical Engineering, Shanghai Jiao Tong University, Shanghai 200000, China
[3]Shanghai Aerospace Control Technology Institute, Shanghai 200000, China

Corresponding author: Xinhua Tang (xinhuatanggnss@163.com)

This work was supported in part by the National Natural Science Foundation of China under Grant 41704025, in part by the Natural Science Foundation of Jiangsu Province under Grant BK20160668, in part by the Aerospace Foundation under Grant 20170869005, in part by the Zhishan Youth Scholar Program of Southeast University, and in part by the Foundation of Shanghai Key Laboratory of Navigation and Location-Based Services.

ABSTRACT As the development of traditional scalar tracking loops, different additional enhancement techniques in a GNSS receiver are proposed to help improve the positioning service quality. Up to now, Kalman-based tracking loop has gained much attention due to its potential superiorities, it has been widely exploited and studied in different specific applications. But meanwhile, there is still a lack of the detailed exploration regarding the Kalman tuning and the fully in-depth analysis and validation. Based on our former related work, an improved mathematical expression of Kalman gain and proper tractable models are proposed to help the analysis of Kalman tuning. An explicit tuning rule is proposed step by step regarding every single parameter involved and the validation is carried out in real experiments by the comparison of different receivers with different configurations. The results verify the proposed tuning rule and advantages of KF-tracking with proper setting. Thanks to the accurate and reliable signal parameter estimation, it can dramatically relieve the burden of the following processing modules, like PVT, RTK and other similar algorithms.

INDEX TERMS GNSS, tracking loop, Kalman filter, carrier-smoothing, Kalman tuning.

I. INTRODUCTION

Originally from the setup of GPS in 1970s, the study of GNSS receiver techniques has been developing from different aspects including the robustness, accuracy, dynamic performances, etc. As a component of paramount importance inside a GNSS receiver, the tracking phase has been always the key research topic in GNSS receiver community. Signal tracking plays an important role to bridge the acquisition and PVT phases and guarantee the continuous positioning service. Especially, in high-precision (PPP, RTK) , GNSS remote sensing and other related applications, the measurements generated from the tracking loop, such as code-pseudorange, phase-pseudorange, Doppler frequency, signal-to-noise density ratio, signal power measurements and other parameters, are fed into the corresponding processing engine to achieve the different objectives. In this sense, it becomes a must to improve the performance of the tracking loop.

A conventional scalar tracking loop consist of a Frequency-Lock-Loop (FLL), a Phase-Lock-Loop (PLL) and a Delay-Lock-Loop (DLL) which are responsible of estimating carrier frequency, phase and code delay of the received signal, respectively. All these lock loops are derived from the similar control loops, perhaps with different orders or loop parameters [1], [2]. In an old standard procedure, the above-mentioned lock loops, including FLL, PLL and DLL, are working independently. In 2000s, different combination of the three lock loops are presented and analyzed [3]. Above all, one typical structure termed as FLL-assisted DLL/PLL becomes a primary option as it can accelerate the converge of frequency estimate and avoid the false-lock [3], [4].

Limited by the theoretical control model of the tracking loop, the performance is always a tradeoff between accuracy and dynamic capabilities. This is also the reason why

The associate editor coordinating the review of this article and approving it for publication was Yuan Zhuang.

empirical values are normally used in parameter setting for different circumstances. Due to the independent working pattern of PLL, DLL and FLL, the inherent relationship between the parameters including carrier frequency, carrier phase and code phase is not well exploited, leading to the limited accuracy of the parameter estimation. In order to improve the accuracy of PVT results, carrier-smoothing algorithm or Kalman filter is needed to do the further processing based on the outputs of tracking loops. More in details, carrier-smoothing is to relate the code phase and carrier phase to improve the estimation accuracy of code phase, which directly decides the accuracy of psuedorange used as the input of the following position calculation [5]. And instead of the simple LS-PVT (least-square based PVT), Kalman filter in PVT engine is employed to fuse the pesudorange and Doppler frequency information, attempting to improve the estimation accuracy of position, velocity and time [6]. The employment of carrier-smoothing or Kalman filter in PVT implies the fact that there is still possibility left to improve the conventional tracking loop.

As mentioned above, in the conventional manner, the estimation of Doppler frequency, code delay and carrier phase are working in a loose-coupled way or sometimes independently. In order to sufficiently exploit the inner relationship between all these unknown parameters, a Kalman-based tracking loop was proposed and analyzed from different perspectives [7], [8]. But most available literature pay more attention to the implementation and application of this advanced structure [9], for instants in the field of geological surveying, the robustness of KF-PLL is taken advantage of to minimize the channel tracking loss probability, and the discontinuities in carrier phase output in scintillation environment [10], [11]. Similarly, in other challenging environments, KF based tracking loop is normally a key option to be considered. For example, EKF-PLL is exploited to improve the tracking performance in circumstance of weak signal [12]–[14], and EKF-based tracking loop aiming at multipath mitigation has been also investigated in [15].

In contrast to the application of KF-based tracking loop, less focus is put on the theoretical analysis and evaluation of the algorithm, generally, KF-PLL is frequently compared with a conventional PLL in terms of equivalent noise bandwidth [16]–[18]. With the comparison of KF-PLL and conventional scalar PLL, an adaptive loop parameter setting rule in a traditional loop can be derived to help improve the performance of traditional PLL in return[19], [20]. The tuning of Kalman filter in KF-based PLL is analyzed in [18] to give an initial insight to the influence of the setting of error covariance, and the influence analysis is more based on simulation and experimental trials. Furthermore in recent years, the practical implementation of KF-based tracking loop in real-time platform is also concerned, KF-based tracking loop is simplified to maintain the comparable complexity with respect to the traditional one, facilitating the practical implementation of KF-based tracking loop [21], [22]. Within one single channel, a KF-based tracking loop can be a perfect

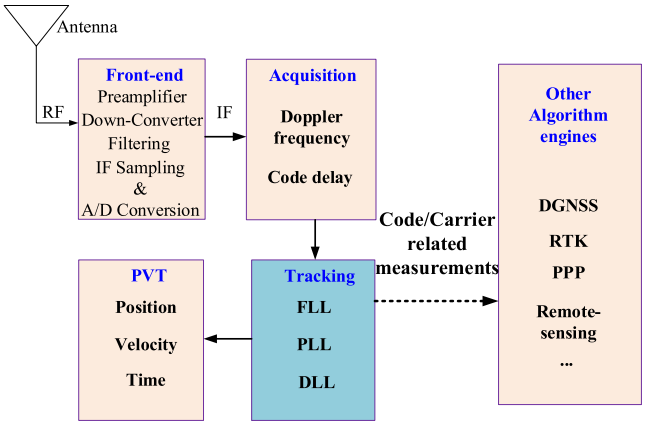

FIGURE 1. The workflow of a GNSS receiver.

solution for the parameter estimation to some degree. When it comes up to the channel level, a vector tracking loop is proposed to change the independent working manner of the traditional tracking channels, briefly, the vector tracking loop is trying to relate the tracking channels in PVT domain[23], essentially the basic ideology behind vector-based tracking loop can be deemed as another promoted level of data fusion.

In summary, most available papers mainly focus on one specific type of tracking enhancement techniques, such as the FLL-assisted DLL/PLL, Carrier-smoothing, Kaman filter in PVT engine and KF-based tracking loop. While minor literature pays attention to the inner relationship or comparison of all these kinds of tracking enhancements that have been proposed and developed during the whole evolution process. Especially in KF-based tracking loop, there is still a lack of the detailed exploration regarding the Kalman tuning and the fully in-depth analysis and validation. In order to clarify the inner relationship between all above-mentioned methods and especially to deeply investigate the full KF-based tracking loop (not just KF-PLL). Firstly in Section 2, a conventional tracking loop is introduced briefly, the common additional filtering algorithms including Carrier-Smoothing and KF in PVT are also simply analyzed. With the prior knowledge of traditional tracking loop design, a Kalman-filter-based tracking loop is analyzed and summarized in theory in Section 3. Additionally, dedicated experiments are carried out to verify the theoretical analysis in Section 4. Finally, future work related to the tracking loop is proposed in the conclusion part.

II. CONVENTIONAL TRACKING LOOP

Tracking loop is a significant part in a GNSS receiver, it bridges the acquisition and PVT phases, keeping track of the received signal transmitted from navigation satellites above in the sky. Additionally, some extended services including RTK, PPP, remote sensing, etc. which bring substantial benefit to the development of our society, are all dependent on the performance of tracking loops.

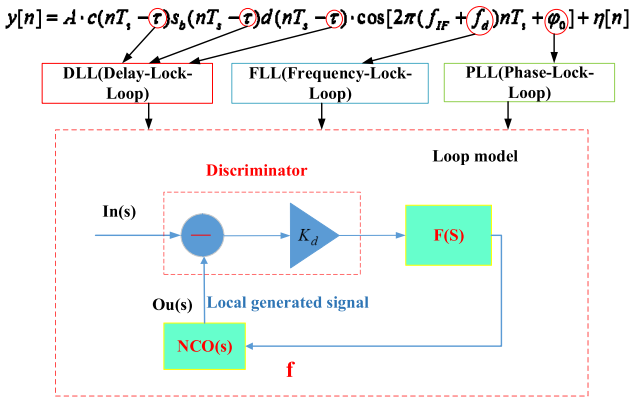

FIGURE 2. The main function of tracking loops.

A. GENERAL DESCRIPTION OF A CONVENTIONAL TRACKING LOOP

As shown in Fig.1, in the signal processing of a GNSS receiver, the transmitted RF (radio-frequency) signal is firstly transferred to IF (intermittent frequency) digital signal for the following processing. The mathematical expression of IF signal can be written as follows:

$$\begin{aligned} y[n] &= A \cdot c(nT_s - \tau)s_b(nT_s - \tau)d(nT_s - \tau) \\ &\quad \cdot \cos[2\pi(f_{IF} + f_d)nT_s + \varphi_0] + \eta[n] \\ n &= 0, 1, 2, 3, 4 \ldots, N-1 \end{aligned} \tag{1}$$

where A is the amplitude of the received signal, f_{IF} is the intermittent frequency, f_d is the Doppler frequency, φ_0 initial carrier phase, T_s is the sampling period, n is the sequence number of the digitalized signal data $c(nT_s - \tau)$ is PRN code, $s_b(nT_s - \tau)$ is sub-carrierČlif there is no subcarrier modulated, then it is set to 1), $d(nT_s - \tau)$ is the navigation message, $\cos[2\pi(f_{IF} + f_d)nT_s + \varphi_0]$ is carrier, $\eta[n]$ is noise term, normally assumed to be an additive White-Gaussian noise.

Once the visible satellites are detected through the acquisition stage, the corresponding rough estimates of Doppler frequency f_d and code phase delay τ for each available satellite will be computed and passed to the following tracking phase as the initialization, meanwhile, the tracking loop will take over the job to track the three unknown parameters continuously as shown in Fig.2.

As illuminated in Fig.2, FLL, PLL and DLL are separately in charge of estimating Doppler frequency, carrier phase and code phase delay. They all share the similar control loop model. Note that "loop filter" in Fig.2 is not always low pass filter, as stated in [24] a better name may have been controller instead of loop filter. The subtraction operation between input parameter and local estimated parameter is achieved by discriminator which is always non-linear. The main purpose of the control loop is to establish the dynamics of the feedback loop and to deliver a suitable control signal to NCO. One of the important parameter in loop design is the loop noise bandwidth defined as.

$$\mathrm{B_{Loop}} = \frac{1}{|\mathrm{H}(0)|^2}\int_0^\infty |\mathrm{H(jw)}|^2 df \tag{2}$$

where H(jw) is the transfer function of the loop.

$$\mathrm{H(s)} = \frac{\mathrm{Ou(s)}}{\mathrm{In(s)}} \tag{3}$$

Another parameter is the damping factor ξ which normally is set to 0.7[24]. The choice of $\mathrm{B_{Loop}}$ and ξ is empirical. Especially for the setting of $\mathrm{B_{Loop}}$, it is always a tradeoff between dynamic performance and accuracy of the control loop. And the order of the loop system depends on the choice of F(s). More details can be referred to in [2] and [24]. Generally, in case of conventional tracking loop, DLL,PLL and FLL are more likely to work independently or in a loose-coupled manner.

B. THE ADDITIONAL ENHANCEMENT BASED ON THE CONVENTIONAL TRACKING LOOP

In order to guarantee the quality of PVT, the estimates from tracking loop normally can't be exploited to do the PVT computation directly. Instead, additional enhancement algorithms are utilized to refine the measurements in further step, such as carrier-smoothing technique [5] and Kalman filter in PVT engine [6]. Both of two aforementioned algorithms can be deemed as additional filtering, only using different methods. This also implies the imperfectness of the traditional tracking loop.

Carrier-smoothing relates the phase-pseudorange measurements and code-pseudorange measurements to refine code-pseudorange estimates as described mathematically as follows [5]:

$$r_{sm}[n] = \frac{1}{M}r_c[n] + (1 - \frac{1}{M})(r_{sm}[n-1] + r_p[n] - r_p[n-1]) \tag{4}$$

where $r_c[n]$ is code-pseudorange, $r_p[n]$ is phase-pseudorange, $r_{sm}[n]$ is the refined code-pseudorange, M is the smoothing window size. It should be noted that the quality of code-pseudorange $r_c[n]$ depends on the accuracy of code phase delay estimates while $r_p[n]$ is related to the carrier phase estimates. In (4), suppose the individual measurement $r_c[n]$ and $r_p[n]$ are uncorrelated, then the variance of the smoothed code-pseudorange $r_{sm}[n]$ can be determined as [25]

$$\mathrm{Var}(r_{sm}) = \frac{1}{2M-1}\mathrm{Var}(r_c) + \frac{2(M-1)^2}{M \cdot (2M-1)}\mathrm{Var}(r_p) \tag{5}$$

in this sense, as the smoothing windows size M increases, the variance of smoothed code-pseudorange is more close to that of the phase-pseudorange, resulting in the improvement in the accuracy of raw code-pseudorange measurement.

On the other hand, in order to improve the accuracy of PVT based on the measurements from tracking loop, a Kalman filter as described in (6) is widely used instead of pure simple

least square method.

$$\begin{bmatrix} \Delta x \\ \Delta y \\ \Delta z \\ \Delta t_u \\ \Delta v_x \\ \Delta v_y \\ \Delta v_z \\ \Delta \dot{t}_u \end{bmatrix}_{k+1} = \begin{bmatrix} 1&0&0&0&T_c&0&0&0 \\ 0&1&0&0&0&T_c&0&0 \\ 0&0&1&0&0&0&T_c&0 \\ 0&0&0&1&0&0&0&T_c \\ 0&0&0&0&1&0&0&0 \\ 0&0&0&0&0&1&0&0 \\ 0&0&0&0&0&0&1&0 \\ 0&0&0&0&0&0&0&1 \end{bmatrix} \begin{bmatrix} \Delta x \\ \Delta y \\ \Delta z \\ \Delta t_u \\ \Delta v_x \\ \Delta v_y \\ \Delta v_z \\ \Delta \dot{t}_u \end{bmatrix}_k + \begin{bmatrix} 0 \\ 0 \\ 0 \\ w_{t_u} \\ w_{v_x} \\ w_{v_y} \\ w_{v_z} \\ w_{\dot{t}_u} \end{bmatrix}_k \tag{6}$$

$$\Delta Z_k = \begin{bmatrix} \rho_1 - \hat{\rho}_1 \\ \rho_2 - \hat{\rho}_2 \\ \cdots \\ \rho_N - \hat{\rho}_N \\ r_1 - \hat{r}_1 \\ r_2 - \hat{r}_2 \\ \cdots \\ r_N - \hat{r}_N \end{bmatrix} \approx \begin{bmatrix} \mathrm{H} & 0 \\ 0 & \mathrm{H} \end{bmatrix} \Delta X_k + V_k$$

$$where: r = \frac{c \cdot (f_r - f_T)}{f_T} + \vec{V}_s \cdot \vec{a}, \mathrm{H} = [\vec{a} \; -1] \tag{7}$$

where $\Delta x \Delta y \; \Delta z$ are the position related correction applied to the predicted Earth-Centered Earth-Fixed (ECEF) coordinates, $\Delta v_x \; \Delta v_y \; \Delta v_z$ are velocity related correction in ECEF. Δt_u is receiver clock bias correction and $\Delta \dot{t}_u$ is clock drift correction. T_c is period of the system, $w_{t_u}, w_{v_x}, w_{v_y}, w_{v_z}, w_{\dot{t}_u}$ are the process noise term for velocity, clock bias and clock drift. ρ is the pseudorange, $\hat{\rho}$ is the prediction value of pseudorange. f_r is the frequency of received signal, f_T is the frequency of transmitted signal. $\vec{V}_s$ is the velocity of the satellite, $\vec{a}$ is a unitary vector pointing from receiver to satellite. The subscripts from 1 to N is the number of the visible satellite. More details can be referred to in [2] and [6].

In summary, carrier-smoothing is proposed to improve the accuracy of pseudorange measurements and Kalman filter in PVT is to improve the accuracy of both pseudorange and pseudorange-rate. They are all developed due to the limited accuracy of measurements from the traditional tracking loops.

III. KALMAN-FILTER-BASED TRACKING LOOP

A KF-based tracking loop integrates DLL,PLL and FLL into one single highly-coupled system, that is to say, the inner relationship between the unknown parameters inside tracking loop, including the Doppler frequency f_d, code phase delay τ and carrier phase θ, is fully exploited. In most previous literature, the KF-PLL is mainly analyzed and compared with the conventional PLL, and an important factor of the loop design termed as equivalent loop noise bandwidth, is derived and compared with the counterpart in a traditional PLL to demonstrate the advantage of KF-PLL. But seldom paper presents a comprehensive investigation of the whole tracking system. Here in this section, instead of one single PLL, the whole tracking loop will be analyzed, in details, distributed noise bandwidths related to multiple parameters are proposed and the influence of KF setting on the parameter estimation is demonstrated both in theory and field experiments.

A. ANALYSIS OF KF-BASED TRACKING LOOP

Practically, there are mainly two options for the implementation of KF-based tracking loop, named as Linear KF-based tracking loop and EKF-based tracking loop as shown in Fig.3. In theory, EKF-based tracking loop has higher sensitivity, but practically, linear KF-based tracking loop has comparable performance with EKF-based one [26]. For simplicity, hereafter, linear KF-based tracking loop is mainly analyzed mathematically.

The Continuous-Update model of a linear KF-based tracking loop is formulated (error-stated) as

$$\begin{bmatrix} \Delta \dot{\tau} \\ \Delta \dot{\theta} \\ \Delta \dot{f} \\ \Delta \dot{\alpha} \end{bmatrix} = \begin{bmatrix} 0&0&\beta&0 \\ 0&0&2\pi&0 \\ 0&0&0&1 \\ 0&0&0&0 \end{bmatrix} \begin{bmatrix} \Delta \tau \\ \Delta \theta \\ \Delta f \\ \Delta \alpha \end{bmatrix} + \begin{bmatrix} 1&\beta&0&0 \\ 0&2\pi&0&0 \\ 0&0&1&0 \\ 0&0&0&1 \end{bmatrix} \begin{bmatrix} w_{code} \\ w_{clc1} \\ w_{clc2} \\ w_{acc} \end{bmatrix} \tag{8}$$

$$Z = \begin{bmatrix} 1&0&0&0 \\ 0&1&0&0 \end{bmatrix} \begin{bmatrix} \Delta \tau \\ \Delta \theta \\ \Delta f \\ \Delta \alpha \end{bmatrix} + v \tag{9}$$

where the system states includes the code-phase error $\Delta \tau$ (unit: chips), the carrier-phase error $\Delta \theta$ (unit: radians), the carrier-frequency error Δf (unit: Hz) and the carrier-frequency rate error $\Delta \alpha$ (unit: Hz/s). the coefficient β is used to convert the units of cycles into units of chips. $\mathbf{w} = [w_{code} \; w_{clc1} \; w_{clc2} \; w_{acc}]^{\mathrm{T}}$ is process noise vector and v is the measurement noise vector.

Currently, the available literature mainly relates the KF-PLL to traditional PLL and compare the equivalent noise bandwidth of PLL. Hereafter based on former work [18], [21], the distributed noise bandwidths concerning carrier phase, Doppler frequency and code phase are derived and analyzed, furthermore, the tuning of KF parameters is also investigated.

With the system described in (8) and (9), the approximation of Kalman gain in steady-state can be expressed as

$$\mathbf{K}_\infty \approx \begin{bmatrix} K_0 & 0 & 0 & 0 \\ 0 & K_1 & K_2 & K_3 \end{bmatrix}^{\mathrm{T}} \tag{10}$$

Additionally, suppose the model of carrier phase error is

$$\Delta\theta(t) = (\Delta\theta_i + 2\pi\,\Delta f \cdot t + \pi\,\Delta\dot{f} \cdot t^2 + \frac{\pi}{3}\Delta\ddot{f} \cdot t^3 + \ldots)u(t) \tag{11}$$

where $u(t)$ is the unit step function. Recalling the measurement update rule of a CU Kalman-Bucy filter, the final update of the states' estimation can be written as [6]

$$\dot{\hat{\mathbf{x}}} = \mathbf{A}\hat{\mathbf{x}} + \mathbf{K}(\mathbf{z} - \mathbf{H}\hat{\mathbf{x}}) \tag{12}$$

From (12), the equivalent control loop of the linear KF-based tracking loop can be illustrated in Fig.4.

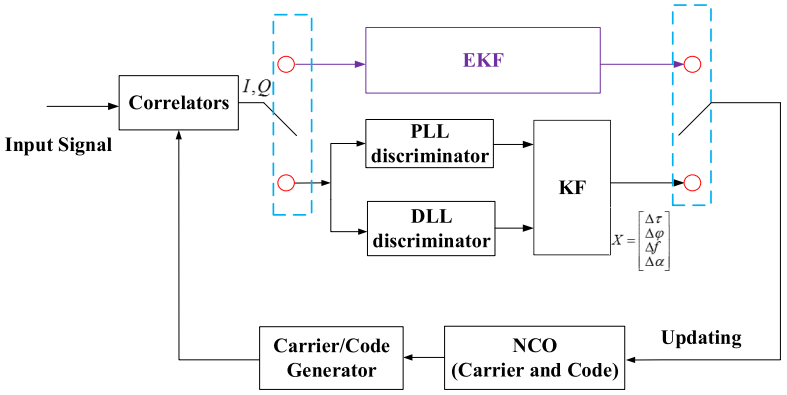

FIGURE 3. The structure of KF-based tracking loop.

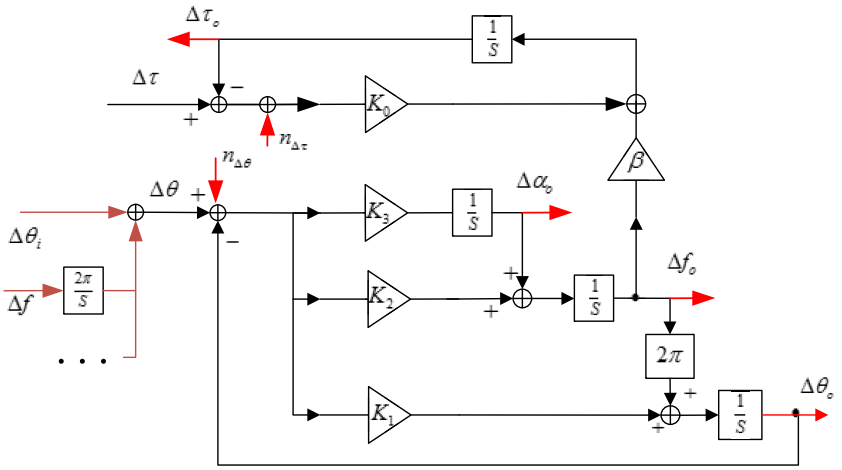

FIGURE 4. The control loop of a linear KF-based tracking loop.

As shown in Fig.4, the following transfer functions with respect to carrier phase error and Doppler frequency can be inferred According to Mason's gain formula (MGF) [27]

$$\frac{\Delta\theta_o(s)}{\Delta\theta(s)} = \frac{K_1 s^2 + 2\pi K_2 s + 2\pi K_3}{s^3 + K_1 s^2 + 2\pi K_2 s + 2\pi K_3} \tag{13}$$

$$\frac{\Delta f_o(s)}{\Delta f(s)} = \frac{2\pi K_2 s + 2\pi K_3}{s^3 + K_1 s^2 + 2\pi K_2 s + 2\pi K_3} \tag{14}$$

With the transfer functions as described in (13) and (14), the equivalent noise bandwidth can be computed separately as [6]

$$B_{n(\Delta\theta)} = \frac{K_1}{4} + \frac{\pi (K_2)^2}{2K_1K_2 - 2K_3} \tag{15}$$

$$B_{n(\Delta f)} = \frac{2\pi (K_2)^2 + K_1K_3}{4K_1K_2 - 4K_3} \tag{16}$$

When it comes to the analysis of code-phase estimation as shown in the upper part in Fig.4, a simplified model termed as frequency-assisted-DLL is proposed as shown in Fig.5.

As shown in Fig.5, $\frac{a}{s+a}$ is a low pass filter where bandwidth a depends on (16), in this sense, the estimation of dynamic component in code phase relies on the frequency aid, while loop gain K_0 can decide the noise bandwidth of $n_{\Delta\tau}(s)$. In details, the contribution of $n_{\Delta\tau}(s)$ in $\Delta\tau_o(s)$ can be computed as

$$\frac{n_{\Delta\tau o}(s)}{n_{\Delta\tau}(s)} = \frac{K_0}{s + K_0} \tag{17}$$

So the corresponding noise bandwidth related to $n_{\Delta\tau}(s)$

$$B_{n_{\Delta\tau}} = K_0 \tag{18}$$

From (15), (16) and (18), it can be observed that the distributed noise bandwidth is related to the tracking loop gains including K_0, K_1, K_2, K_3 as shown in Fig.4. Compared with a traditional tracking loop, the main advantage of Kalman-based tracking loop can be generally attributed to the Kalman gains which are always adaptive and more physically reasonable. As mentioned before, the previous literature mainly analyzed the benefit brought by the loop gains in PLL with less emphasis on the setting of Kalman filter parameters and the corresponding influence.

B. THE DETAILED SETTING OF KALMAN PARAMETERS

In a Kalman system, the Kalman gains actually depends on various parameters including initial error covariance, system state noise covariance, measurement noise covariance. Based on our former work [21], the improved approximation can be

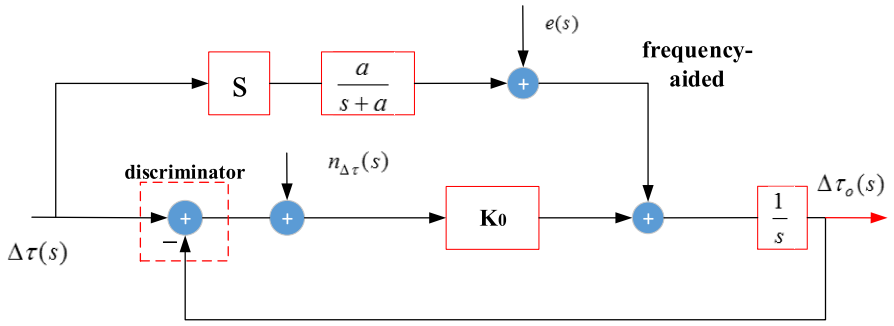

FIGURE 5. The simplified model of code-phase estimation in a Kalman-based tracking loop.

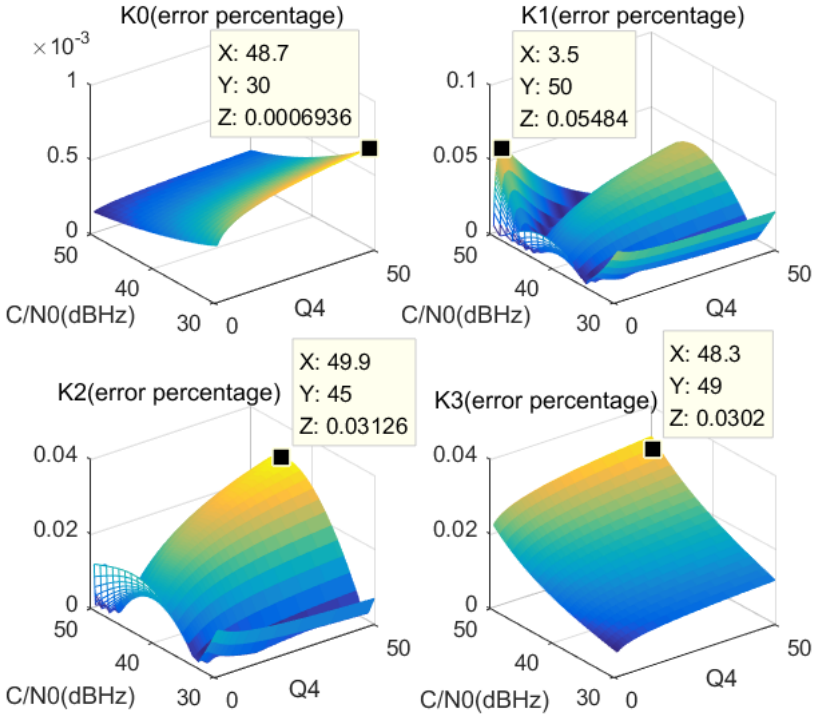

FIGURE 6. The error percentage of Kalman gain expression in (19).

obtained as follows to facilitate the computation of Kalman gains in steady state.

$$K_0 = \sqrt{\frac{Q_1}{R_1}}$$

$$K_3 = \sqrt{\frac{Q_4}{R_2}}$$

$$K_2 = \left(\sqrt[3]{-\frac{q}{2}+\sqrt{\left(\frac{q}{2}\right)^2+\left(\frac{p}{3}\right)^3}}+\sqrt[3]{-\frac{q}{2}-\sqrt{\left(\frac{q}{2}\right)^2+\left(\frac{p}{3}\right)^3}}\right)\cdot E_s$$

$$K_1 = \frac{\left(K_2^2 - \frac{Q_3}{R_2}\right)\cdot\pi}{\sqrt{\frac{Q_4}{R_2}}} \times \left(\begin{array}{l} where\ q = -\dfrac{4\cdot Q_4}{\pi R_2};\ p = -\dfrac{2\cdot Q_3}{R_2} \\ E_s = 1 + 0.004\cdot\left(10\cdot\log_{10}\left(\dfrac{1}{2\cdot R_2}\right) - 30\right) \end{array}\right) \quad (19)$$

Q_1, Q_2, Q_3, Q_4 are four elements of the process noise covariance in the system described in (8) defined as $\mathbf{Q} = E[\mathbf{w}\mathbf{w}^{\mathrm{T}}] = \mathrm{diag}([Q_1, Q_2, Q_3, Q_4])$, where the 'diag' operator indicates a diagonal matrix with the specified major diagonal. R_1, R_2 are the two components of measurement noise covariance in (9) defined as $\mathbf{R} = \mathrm{diag}([R_1, R_2]) = E[\mathbf{v}\mathbf{v}^{\mathrm{T}}]$, depending on the variance of discriminators' outputs. Regarding the approximation in (19), it should be noted that the solutions for K_0, K_1, K_2 are nearly closed-form, while the expression of K_2 partially involves mathematical fitting processing shown as the scale factor E_s. The advantage of (19) compared with former expression in [21] is the higher accuracy and wider scope as shown in Fig.6

From Fig.6, it can be observed that the maximum error percentages for K_0, K_1, K_2, K_3 are separately 0.07%, 5.4%, 3.1% and 3% in a rational large scope., in which Signal-to-Noise density is located in [30 −50] dBHz and the value of varies from 0.5 to 50 (The meaning will be explained later

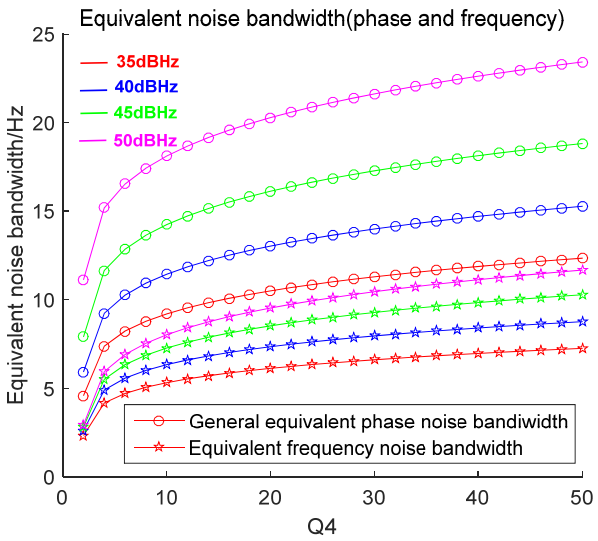

FIGURE 7. The equivalent noise bandwidth with respect to phase and frequency.

in the setting of Q_4). In this paper, the detailed derivation of Kalman gain as (19) is not the key topic, hereafter the close-form solutions of K_0 and K_3 will be exploited to help the setting of Kalman parameters. For K_0 and K_3, the error of approximation is very small which can be ignored to some degree. While for K_1, K_2, there is certain error involved which is around several percentage of the true value. But it won't affect the following analysis.

The setting of Kalman filter parameters is always heuristic or empirical, hereafter, explicit setting of parameters are discussed in the following steps.

1. Firstly, the setting of measurement noise covariance associated to the code-phase error $\Delta\tau$ and carrier-phase $\Delta\theta$, $\mathbf{R} = \text{diag}([R_1, R_2])$ can be computed directly [2], [6]

$$R_1 \approx \sigma_{\Delta\tau}^2 \cdot T = \frac{d_o T}{4T \cdot \left(C/N_0\right)} \left(1 + \frac{2}{(2-d_o)T \cdot \left(C/N_0\right)}\right)$$
$$R_2 \approx \sigma_{\Delta\theta}^2 \cdot T = \frac{T}{2T \cdot \left(C/N_0\right)} \left(1 + \frac{1}{2T \cdot \left(C/N_0\right)}\right) \quad (20)$$

where $\sigma_{\Delta\tau}$, $\sigma_{\Delta\theta}$ are the noise variance of code phase and carrier phase discriminators separately, T is the integration time, d_o is the spacing between early and late replica codes and C/N_0 is the carrier-to-noise density ratio.

2. Secondly, from the perspective of physical meaning, Q_2 and Q_3 are related to the receiver's clock noise and can be obtained from the Allan Variance h-parameters of the user's clock model, i.e. the white noise frequency coefficient h_0 (s2/Hz) and frequency random walk coefficient h_{-2} (1/Hz) [6], [28], in case of VCTCXO oscillator, we get the following results in terms of noise covariance $Q_2 = 10^{-4}$, $Q_3 = 10^{-2}$. It needs to be noted that the setting of $\mathbf{Q}$ with accuracy up to the order of magnitude is enough for the system.

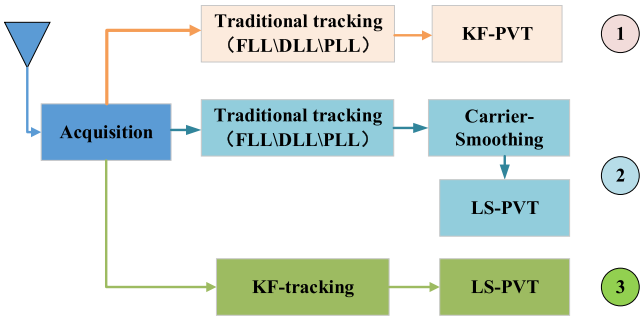

FIGURE 8. The receivers with different configurations.

3. The setting of Q_4 can be analyzed from the perspective of Steady State Error (SSE) of the transfer function. For system as described in (13), the SSE caused by constant and frequency rate term in (11) is zero, the SSE related to frequency jerk term can be analyzed in (21).

$$E_{SSE} = \lim_{s\to 0} s\left(1 - \frac{\Delta\theta_O(s)}{\Delta\theta(s)}\right) \cdot \frac{6 \cdot \frac{\pi}{3}\Delta\dddot{f}}{s^4} = \frac{\Delta\dddot{f}}{K_3} = \frac{\Delta\dddot{f}\sqrt{R_2}}{\sqrt{Q_4}} \quad (21)$$

From (20), it can be observed that

$$R_2 \approx \frac{1}{2 \cdot \left(C/N_0\right)} \quad (22)$$

Furthermore, if under the requirement that SSE be equal to 0.01 phase cycles, considering the dynamic range as $\Delta\dddot{f} = 0 - 10g/s$ and $\left(C/N_0\right)_{\text{dB}} = 40\text{dBHz}$, the setting of Q_4 varies from 0 to 50 according to the dynamic stress. In low-dynamic case, such as the case of daily car driving, Q_4 is normally set to 1.

The setting of Q_4 can decide the dynamic threshold of the system, as in old fashion, the equivalent of noise bandwidth with respect to different Q_4 and signal-to-noise density is plotted in Fig.9, generally, the equivalent noise bandwidth increase as Q_4 becomes larger. In Fig.9, a concept termed as 'distributed noise bandwidth' is proposed, as it is shown there are two different noise bandwidths, one is set for the general phase noise (as PLL) and the other is dedicated to frequency noise. Obviously, the state parameters in KF-tracking hold different equivalent noise bandwidth, taking Fig.9 for example, the noise bandwidth of frequency are much smaller than that of general phase, and as Q_4 increases, the change in frequency noise bandwidth is still smaller, which means it this case enlarging the general system noise bandwidth will not affect the frequency estimate accuracy so much.

4. The last important parameter that needs to be carefully set is Q_1, firstly, according to (20), it can be obtained that $R_1 \approx d_o \Big/ \left(4 \cdot \left(C/N_0\right)\right)$. Additionally based on (18), the setting of K_0 depends the value of bandwidth $B_{n_{\Delta\tau}}$, according to the model shown in Fig.5, it has been analyzed that the estimate of dynamic terms in code phase fully depends on

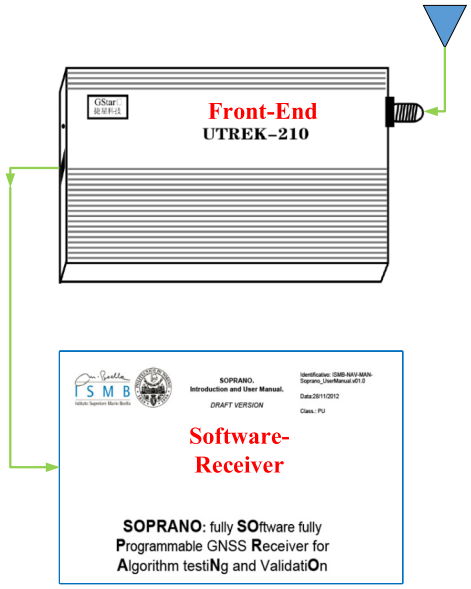

FIGURE 9. Setup of static experiments.

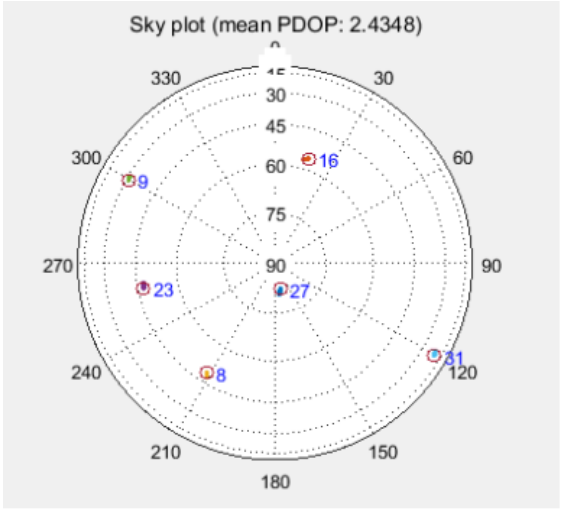

FIGURE 10. The available GPS satellites and mean GDOP.

the frequency aide from carrier phase tracking part, in other words, $B_{n_{\Delta\tau}}$ can be set to very small to suppress the possible large variance of $n_{\Delta\tau}(s)$. From the comparison as shown in Fig.11 in the next section, it can be determined that the suitable magnitude order of value for $B_{n_{\Delta\tau}}$ can be better set smaller than 0.01Hz assuming signal-to-noise density ratio is around $\left(C/N_0\right)_{\text{dB}} = 40\text{dBHz}$.

IV. THE COMPARISON BETWEEN KF-BASED TRACKING LOOP AND TRADITIONAL TRACKING LOOP

In order to give a deep insight into the superiority of KF-based tracking loop from the angle of practical performance, the receivers with different configuration as shown in Fig.8 are proposed and evaluated. Meanwhile, the setting of Kalman parameters in section 3.2 is further discussed and verified.

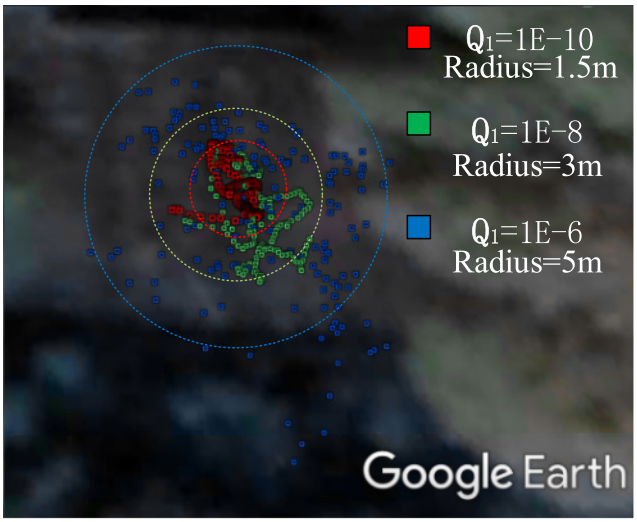

FIGURE 11. The results with different Q_4 setting in configuration 3.

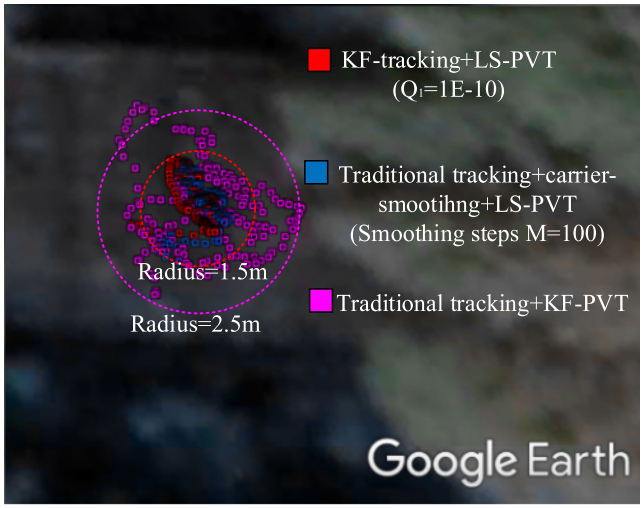

FIGURE 12. The positioning results from configuration 1, 2 and 3.

A. THE COMPARISON IN A STATIC SCENARIO

As shown in Fig.8, three different configurations are proposed for the following analysis to explore the advantage of KF-tracking and more in the setting of KF parameters. In order to verify the inner relationship between KF-tracking and traditional counterparts, firstly the experiments in static case are carried out. The setup mainly includes both hardware and software parts, in hardware, a front-end with intermediate frequency equal to 3.996Ghz is mounted to collect data, in signal processing part, all the aforementioned receivers with three different configurations are further implemented in the frame of SOPRANO, a basic GNSS software receiver from NavSAS group in ISMB Italy.

The first scenario is a static case, an antenna is mounted on the top of a building to receive the signal from the visible satellites (shown in Fig.10) for about 200 seconds, and the software receiver with different configuration is used to process the digital IF (intermediate frequency) data.

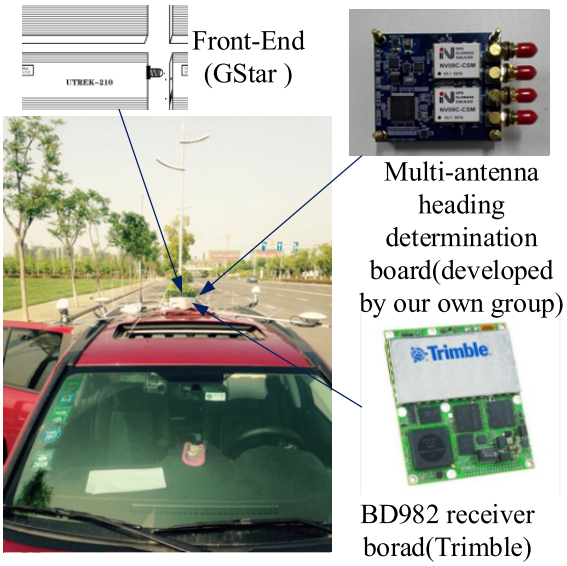

FIGURE 13. Setup of dynamic experiments.

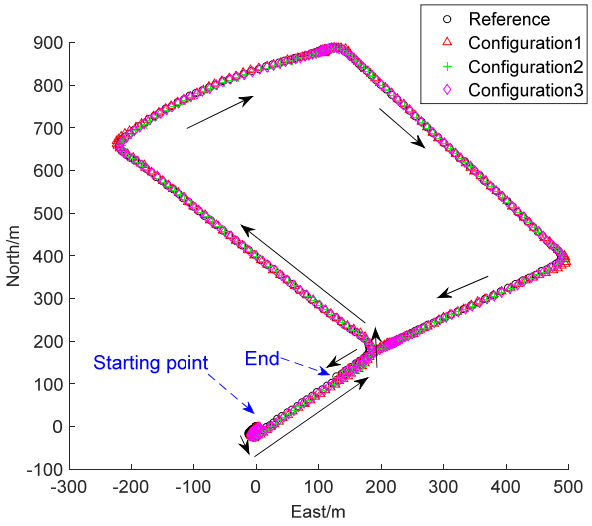

FIGURE 14. The positioning results from configuration 1, 2 and 3 and reference.

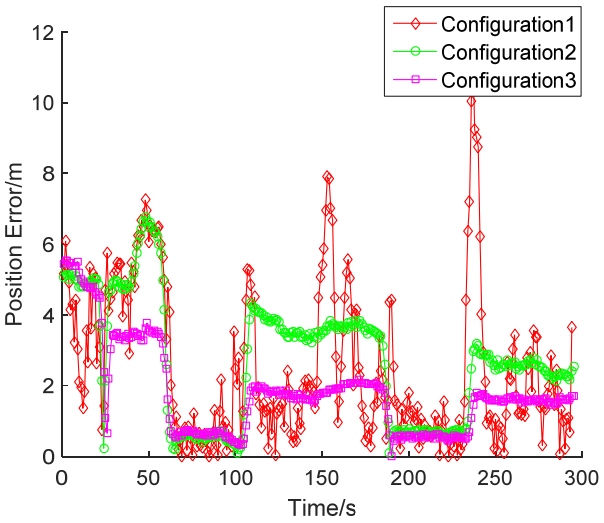

FIGURE 15. The positioning error of the receiver with three different configurations (Horizontal).

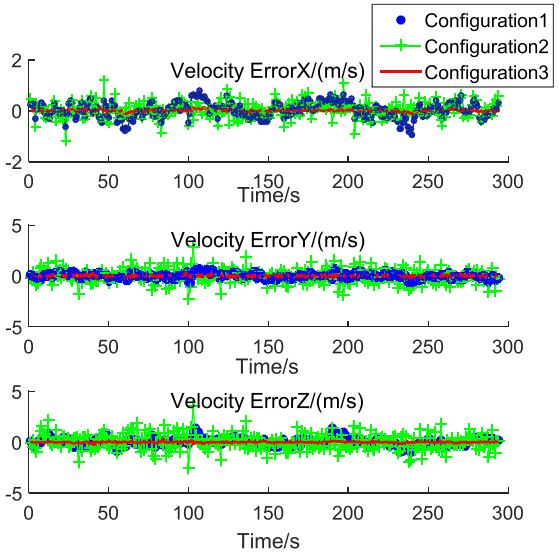

FIGURE 16. The velocity error (in ECEF) of the receiver with three different configurations.

Recalling the setting of Q_1, it is not straightforward as Q_2 and Q_3, Q_1 is related to $B_{n_{\Delta\tau}}$, the equivalent noise bandwidth for low-dynamic component inside the code phase. Here in the first comparison, the positioning results of different Q_1 is shown in Fig.11, obviously as Q_1 increase from 1e-10 to 1e-6, the variance of positioning results increases.

Furthermore recalling (5) and (18), essentially both of carrier-smoothing and the setting of mean to weaken the noise influence in code measurements by decrease the noise bandwidth. Then, with the same IF data, the positioning results between the three different configurations (shown in Fig.8) are shown in Fig.10.

As shown in Fig.12, specifically, in configuration 3, Q_1 is set to 1e-10. In configuration 2, smoothing steps M = 100 which is commonly used in a wide variety of receiver products. It can be observed that the positioning results between configuration 2 and 3 are comparable, which is better than that of configuration 3. In this sense, in daily movement dynamic cases, the state noise covariance can be set as $\mathbf{Q} = E[\mathbf{w}\mathbf{w}^{\mathrm{T}}] = \mathrm{diag}\left([10^{-10},\ 10^{-4},\ 10^{-2},\ 1]\right)$.

B. THE COMPARISON IN A TYPICAL DYNAMIC SCENARIO

In order to verify the parameter setting and inner relationship between three different configurations shown in Fig.8, a typical car experiment is carried out, the car is equipped with front-end, BD982 receiver used as reference, and a heading reference system designed by ourselves. Here, the BD982 receiver supports multi GNSS constellation and is working under SBAS mode with the positioning accuracy up to 0.5 meter. The front-end collects the available GPS signal, meanwhile, the reference results are also logged.

TABLE 1. The statics of positioning and velocity errors.

Configuration	Mean value of Positioning error(absolute value)	Square root of variance	Mean value of velocity error(absolute value in X,Y,Z under ECEF)	Square root of variance (in X,Y,Z under ECEF))
Traditional tracking +KF-PVT(1)	2.58m	3.24m	0.24m/s, 0.21m/s, 0.31m/s,	0.30m/s, 0.25m/s, 0.38m/s
Traditional tracking +CS+LS-PVT(2)	2.74m	3.43m	0.24m/s, 0.53 m/s, 0.60m/s	0.32m/s, 0.69 m/s, 0.78m/s
KF-tracking+ LS-PVT(3)	1.81m	2.21m	0.028 m/s, 0.041m/s, 0.039m/s	0.039 m/s, 0.059m/s, 0.061m/s

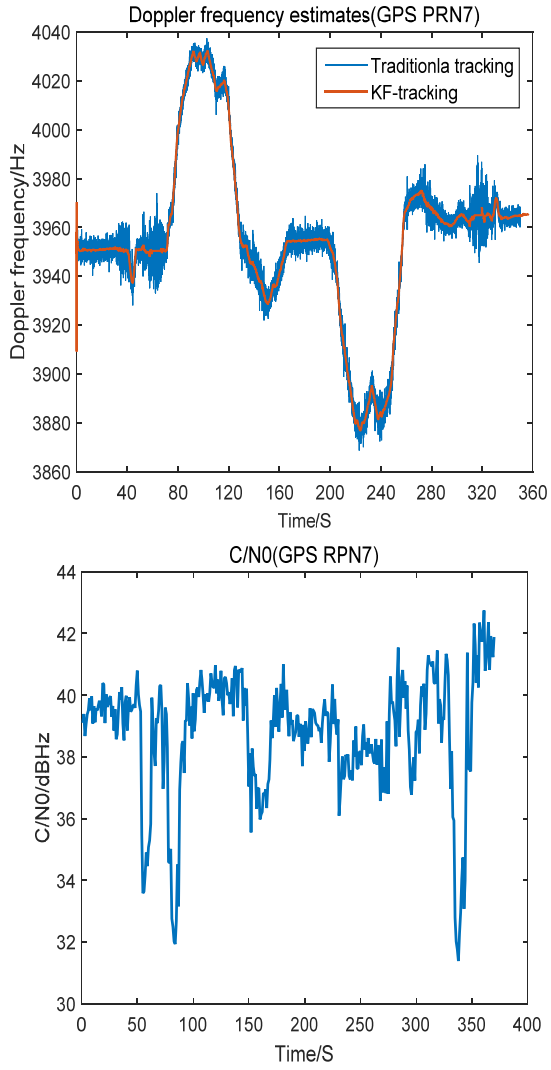

FIGURE 17. The Doppler frequency estimates in the dynamic experiment.

The software receivers with three different configurations are used to do the post-processing. The positioning trajectories are shown in Fig.14.

In Fig.14, all the configurations can work well in this environment, with respect to the reference, the positioning errors (absolute value) are shown in Fig.15, and the mean value of positioning errors for different configurations are listed in Table.1. Similarly, regarding the velocity estimates, the results are shown in Fig.16 and Table1.

As the results show, in terms of positioning accuracy in dynamic case, even with the simple PVT engine, that is LS-PVT, configuration 3 still can achieve the best performance compared with the other two configurations.

1. Differently from static case, Configuration 2 with Carrier-Smoothing can't achieve comparable performance with Configuration 3. The reason for that is due to the help of frequency aide from the lower part in Fig.4.

2. Even though configuration 2 and 3 have similar performance in positioning estimate, but configuration 1 performs much better in terms of velocity estimates, that is because carrier-smoothing can only filter the code phase measurement while configuration 1 do filtering both in code phase and frequency estimates.

3. The high accuracy of velocity estimates in configuration 3 is due to the more physical and tractable parameter setting in KF-tracking part, leading to the accurate Doppler frequency as shown in Fig.17

4. Configuration 3 outperforms the other two configurations both in positioning and velocity estimates, this should be attributed to the KF-tracking. It can directly supply the accurate code phase, carrier phase and frequency estimates to relieve the stress of the post-processing part including PVT, RTK and so on.

V. CONCLUSION

The paper explicitly presents the inner relationship between advanced KF-tracking and traditional scalar tracking with additional enhancement. In details, the parameter setting rule as proposed in this paper can be equivalently related to the available enhancement techniques including Carrier-Smoothing and KF in PVT. In order to give a fully insight into the Kalman tuning, the setting rule is analyzed in proper

mathematically tractable models and verified in practical experiments. In summary, the measurement covariance **R** can be computed directly, while in state noise covariance, Q_2 and Q_3 are decided by the clock model, Q_1 is related to the target noise bandwidth of low-dynamic code phase component, it functions similarly as Carrier-Smoothing, and Q_4 decides the dynamic threshold of the system. At the same time, an improved simplified mathematical expression of Kalman gain in (19) is also given to facilitate the in-depth analysis and implementation of this advanced tracking loop in practical platform. As verified both in the analysis and experiments, the KF-tracking with proper setting can supply the accurate the reliable frequency estimate, code phase estimate and carrier phase estimate, which dramatically relieve the burden of following processing modules, such as PVT, RTK and other similar dedicated algorithms relying on the information source from tracking loops.

REFERENCES

[1] R. Jaffe and E. Rechtin, "Design and performance of phase-lock circuits capable of near-optimum performance over a wide range of input signal and noise levels," *IRE Trans. Inf. Theory*, vol. 1, no. 1, pp. 66–76, Mar. 1955.

[2] E. D. Kaplan and C. J. Hegarty, "Satellite signal acquisition, tracking, and data demodulation," in *Understanding GPS: Principles and Applications*. Boston, MA, USA: Artech House, 2006, pp. 153–242.

[3] A. A. López-Salcedo, J. A. Del Peral-Rosado, and G. Seco-Granados, "Survey on robust carrier tracking techniques," *IEEE Commun. Surveys Tuts.*, vol. 16, no. 2, pp. 670–688, 2nd Quart., 2014.

[4] P. A. Roncagliolo, J. G. García, and C. H. Muravchik, "Optimized carrier tracking loop design for real-time high-dynamics GNSS receivers," *Int. J. Navigat. Observ.*, vol. 2012, Mar. 2012, Art. no. 651039. doi: 10.1155/2012/651039.

[5] Letizia Lo Presti and Monica Visinitin, "Can you list all the properties of the carrier-smoothing filter?" Inside GNSS, Jul. 2015. [Online] Available: https://insidegnss.com/auto/julyaug15-SOLUTIONS.pdf

[6] R. G. Brown and P. Y. C. Hwang, *Introduction to Random Signals and Applied Kalman Filtering*, 3rd ed. New York, NY, USA: Wiley, 1997.

[7] B. W. Parkinson, P. Enge, P. Axelrad, and J. J. Spilker, Jr., *Global Positioning System: Theory and Applications*. Washington, DC, USA: AIAA, 1996.

[8] J.-H. Won, D. Dötterböck, and B. Eissfeller, "Performance comparison of different forms of Kalman filter approaches for a vector-based GNSS signal tracking loop," *Navigat., J. Inst. Navigat.*, vol. 57, no. 3, pp. 185–199, 2010.

[9] Y. Cheng, Q. Chang, H. Wang, and X. Li, "A two-stage Kalman filter-based carrier tracking loop for weak GNSS signals," *Sensors*, vol. 19, no. 6, p. 1369, 2019.

[10] V. Barreau, W. Vigneau, C. Macabiau, and L. Deambrogio, "Kalman Filter based robust GNSS signal tracking algorithm in presence of ionospheric scintillations," in *Proc. 6th ESA Workshop Satellite Navigat. Technol. (Navitec) Eur. Workshop GNSS Signals Signal Process.*, Dec. 2012, pp. 1–8.

[11] P. Sun, X. Tang, Y. Huang, and G. Sun, "Wavelet de-noising Kalman filter-based Global Navigation Satellite System carrier tracking in the presence of ionospheric scintillation," *IET Radar Sonar Navigat.*, vol. 11, no. 2, pp. 226–234, Feb. 2017.

[12] Z. He and M. Petovello, "Performance comparison of Kalman filter and maximum likelihood carrier phase tracking for weak GNSS signals," in *Proc. Int. Conf. Indoor Positioning Indoor Navigat. (IPIN)*, Banff, AB, Canada, Oct. 2015, pp. 1–8.

[13] M. L. Psiaki and H. Jung, "Extended Kalman filter methods for tracking weak GPS signals," in *Proc. ION GPS*, Portland, OR, USA, Sep. 2002, pp. 1–15.

[14] N. I. Ziedan and J. L. Garrison, "Bit synchronization and Doppler frequency removal at very low carrier to noise ratio using a combination of the Viterbi algorithm with an extended Kalman filter," in *Proc. ION GPS/GNSS*, Portland, OR, USA, Sep. 2003, pp. 1–12.

[15] G.-I. Jee, H. S. Kim, Y. J. Lee, and C. G. Park, "A GPS C/A code tracking loop based on extended Kalman filter with multipath mitigation," in *Proc. ION GPS*, Portland, OR, USA, Sep. 2002, pp. 446–451.

[16] X. Niu, B. Li, N. I. Ziedan, W. Guo, and J. Liu, "Analytical and simulation-based comparison between traditional and Kalman filter-based phase-locked loops," *GPS Solutions*, vol. 21, no. 1, pp. 123–135, 2017.

[17] J.-H. Won, T. Pany, and B. Eissfeller, "Characteristics of Kalman filters for GNSS signal tracking loop," *IEEE Trans. Aerosp. Electron. Syst.*, vol. 48, no. 4, pp. 3671–3681, Oct. 2012.

[18] X. Tang, G. Falco, E. Falletti, and L. Lo Presti, "Theoretical analysis and tuning criteria of the Kalman filter-based tracking loop," *GPS Solutions*, vol. 19, no. 3, pp. 489–503, 2015.

[19] J.-H. Won and B. Eissfeller, "A tuning method based on signal-to-noise power ratio for adaptive PLL and its relationship with equivalent noise bandwidth," *IEEE Commun. Lett.*, vol. 17, no. 2, pp. 393–396, Feb. 2013.

[20] J.-H. Won, "A novel adaptive digital phase-lock-loop for modern digital GNSS receivers," *IEEE Commun. Lett.*, vol. 18, no. 1, pp. 46–49, Jan. 2014.

[21] X. Tang, G. Falco, E. Falletti, and L. L. Presti, "Complexity reduction of the Kalman filter-based tracking loops in GNSS receivers," *GPS Solutions*, vol. 21, no. 2, pp. 685–699, 2017.

[22] N. Pastori, L. Siniscalco, A. Zin, A. Ferrario, and A. Emmanuele, "Relief of computational burden for a robust carrier tracking based on a kalman filter implementation," in *Proc. 8th ESA Workshop Satellite Navigat. Technol. Eur. Workshop GNSS Signals Signal Process.*, Dec. 2016, pp. 1–8.

[23] X. Tang, G. Falco, E. Falletti, and L. Lo Presti, "Performance comparison of a KF-based and a KF+VDFLL vector tracking-loop in case of GNSS partial outage and low-dynamic conditions," in *Proc. 7th ESA Workshop Satellite Navigat. Technol. Eur. Workshop GNSS Signals Signal Process. (NAVITEC)*, Noordwijk, The Netherlands, Dec. 2014, pp. 1–8.

[24] P. L. Kazemi, "Development of new filter and tracking schemes for weak GPS signal tracking," Ph.D. dissertation, Dept. Eng., Aerosp., Eng., Electron. Elect., Univ. Calgary, Calgary, AB, Canada, May 2010.

[25] M. Orejas, J. Skalicky, M. Pfleger, and J. Samson, "Smoothed pseudo-range performance prior to steady-state operations," in *Proc. Navitec*, Noordwijk, The Netherlands, Dec. 2016, pp. 1–6.

[26] X. Tang, G. Falco, E. Falletti, and L. Lo Presti, "Practical implementation and performance assessment of an Extended Kalman Filter-based signal tracking loop," in *Proc. ICL*, Turin, Italy, Jun. 2013, pp. 1–6.

[27] W. Bolton, *Newnes Control Engineering Pocket Book*. Oxford, U.K.: Newnes, 2016.

[28] C. O'Driscoll, M. G. Petovello, and G. Lachapelle, "Choosing the coherent integration time for Kalman filter-based carrier-phase tracking of GNSS signals," *GPS Solutions*, vol. 15, no. 4, pp. 345–356, 2011.

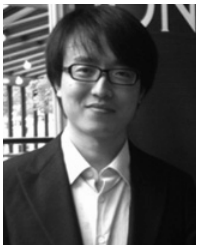

XINHUA TANG received the Ph.D. degree from the Politecnico di Torino, Italy. He was with the Istituto Superiore Mario Boella (ISMB), Italy, in 2014. He is currently an Assistant Professor with Southeast University, Nanjing, China. His current research interests include the development of advanced GNSS techniques, integration systems, and autonomous systems.

XIN CHEN is currently an Associate Professor with Shanghai Jiao Tong University. His research interests include multipath signal processing and integrated navigation systems.

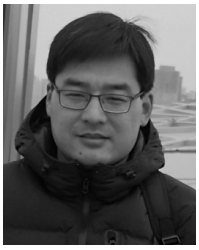

ZHONGHAI PEI is currently a Technique Leader with the Navigation Department, Shanghai Aerospace Control Technology Institute. His research interests include the receiver techniques, RTK, INS navigation systems, and rocket control theory.

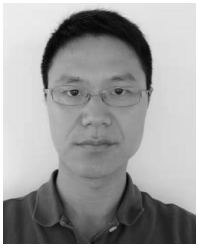

PENG WANG is currently a Senior Researcher with the Navigation Department, Shanghai Aerospace Control Technology Institute. His research interests include GNSS navigation systems and rocket control theory.